Transcriptomic signatures of disease tolerance and environmental persistence in a mosquito-microsporidian system

Luís M. Silva [1,2 *]

[1] Institute of Biology, University of Neuchâtel, Neuchâtel, Switzerland

[2] Department of Zoology, University of British Columbia, Vancouver, Canada

* Corresponding author: luis.silva@ubc.ca

ORCID: 0000-0002-8203-4006

Word count without tables, figures and references: 5,355 words.

Abstract

Parasite life histories are expected to shape virulence and transmission, but the host programmes involved are largely unknown. Experimental evolution and RNA-seq were combined in a mosquito-nicrosporidian system, *Anopheles gambiae*-*Vavraia culicis,* to test how evolved parasite strategies alter host gene expression. A mosquito population was infected with parasite lineages selected for *early* or *late* transmission and compared with infections by an unselected *reference* parasite and with *uninfected* controls. Whole-body transcriptomes were all sampled at a common sporulating stage of infection. A core infection signature was identified by contrasting *reference* infections with *uninfected* mosquitoes. Against this baseline, *early* and *late* parasites generated distinct, partly overlapping expression profiles. Network analysis revealed modules whose activity tracked infection background and estimates of virulence and parasite load. One module was negatively associated with virulence and enriched for genes involved in damage limitation and tissue integrity, consistent with a disease tolerance programme. A second was positively associated with environmental persistence and enriched for genes that condition the replication and release environment, indicating that host pathways can influence the robustness of transmission stages. These findings link parasite life history, host tolerance and environmental persistence and highlight molecular targets for eco-evolutionary studies of vector-borne disease.

Introduction

Parasites have a diverse array of strategies and life histories, many of which are constrained by how they move between hosts and persist within them. Virulence, the reduction in host fitness caused by infection, emerges from interactions between host defence and parasite strategy, rather than being a fixed property of the parasite alone [1, 2]. Hosts can reduce infection costs by limiting parasite load (resistance) or by limiting the damage caused by the infection or the immune response to it (tolerance) [3–6]. Tolerance can arise through damage repair, metabolic reallocation, or maintenance of barrier integrity, and is therefore expected to leave a different transcriptional footprint from classical resistance responses (centred on parasite killing) [7–10]. Parasites, in turn, can increase virulence either by exploiting host resources more strongly (host exploitation) or by investing in factors that damage hosts independently of load (per-parasite pathogenecity; for instance, toxins) [2, 3, 11, 12]. Classical models often compress this complexity into a single trade-off between transmission rate and virulence [13, 14]. Yet, empirical work shows that such simplified expectations only partly capture how virulence evolves in nature, especially when different parts of the transmission cycle are under selection as well [15–18].

For parasites with environmental stages, resources must be allocated between replication within hosts and the production of infective stages that survive and remain infective in the environment outside the host [18–20]. This creates space for trade-offs between within-host adaptation and environmental

persistence, which, in turn, translates into differences in virulence [21–23]. At the same time, hosts experience infections against a background of their own life histories [24–26]. When infection shortens expected lifespan, hosts may shift investment from somatic maintenance towards early reproduction, a pattern described as terminal investment [27–29]. These eco-evolutionary feedbacks between parasite life history, host life history and environmental persistence are central to infection outcomes, yet the host transcriptional programmes underlying resistance, tolerance, and transmission remain poorly studied, particularly in vector hosts. In vector systems, this life history overlap is especially relevant. Several vector-borne parasites, such as *Plasmodium*, depend on mosquitoes that survive long enough to complete their life cycle. Selection is therefore expected to favour co-infecting parasites that persist within the host for longer.

The microsporidian parasite *Vavraia culicis* [30] and the mosquito host *Anopheles gambiae* provide a natural model for studying these links. *V. culicis* is an obligate intracellular parasite that infects mosquito larvae, proliferates through larval and adult stages and is (mostly) transmitted when infected adults die and release spores into water [31]. The parasite must therefore balance rapid growth and spore production within mosquitoes against the durability and infectivity of spores in the aquatic environment.

An. gambiae is a major malaria vector whose immunity, physiology and life history under infection are particularly relevant for transmission biology. In such vectors, tissues that parasites must cross, infect or exploit, such as the gut and reproductive organs, act as evolved filters that can amplify, dampen or delay transmission. For *Plasmodium*, for example, the mosquito midgut epithelium and complement-like factor TEP1 kill a substantial fraction of invading ookinetes, making this epithelial barrier a major determinant of *An. gambiae* vectorial capacity [32]. Similar work on arboviruses has shown that midgut and salivary-gland barriers strongly modulate whether virions reach the saliva [33, 34]. Still, very little is known about the host genes and programmes that condition the quality, replication and environmental persistence of transmission stages in environmentally transmitted parasites, despite theory predicting that host traits and environmental survival jointly shape transmission and virulence [22].

Experimental evolution of *V. culicis* in *An. gambiae* has shown that parasite life history can evolve rapidly under selection on the timing of transmission [12]. Lineages selected for spores from hosts that died early in infection (hereby *early*) and from hosts that died late (*late*) were derived from an unselected reference population (*reference*) and maintained for multiple generations. This selection produced multiple correlated changes: *late* lines exploit hosts more strongly, reach higher chronic burdens and are more virulent than *early* lines, but their spores lose infectivity more quickly outside the host; *early* lines are less virulent and achieve lower burdens, but produce spores that persist longer [12, 35, 36]. The same lines also differ in the host life-history responses they elicit, including development time, the timing of reproduction and the balance between reproduction and somatic maintenance [12].

These findings show that selection on parasite transmission time reshapes parasite exploitation, virulence, environmental persistence, and host life history. Still, they do not yet reveal how these changes are encoded in host gene expression.

RNA sequencing (RNA-seq) can bridge this gap by revealing which host pathways are affected under different parasite strategies and which host programmes covary with evolved parasite traits. In vector systems, this matters for at least three reasons. First, it shows whether parasites mainly trigger classical immune pathways or instead push hosts into alternative strategies. Second, it identifies host genes and gene sets that track key parasite traits, including virulence, exploitation and environmental persistence, highlighting potential points of control over disease outcomes and transmission. Third, it provides a mechanistic link between parasite life history and host response in a tractable microsporidian–mosquito model, offering principles that are likely to generalize to more complex vector– and non-vector parasite systems.

The present study uses experimental evolution and RNA-seq to examine how evolved parasite life histories are encoded in the *An. gambiae* transcriptome **(Fig. 1)**. A Kisumu mosquito population was exposed to one of four treatments: *uninfected* controls, infection with the *unselected* reference parasite, and infection with *early*- and *late*-selected *V. culicis* lines. Whole-body transcriptomes of adult females were measured on day 10, when infections of all parasite lineages had reached the end of the infective cycle and started sporulating [12]. In this experiment, replication occurred at two levels: within lineages, through four independent pools of mosquitoes per line, and across lineages, through five independently evolved *early* lines and *five* late lines. This design permits evolutionary inferences from replicated *early*- and *late*-regime samples, while using the single *reference* and *uninfected* lines as physiological anchors for infection and baseline expression.

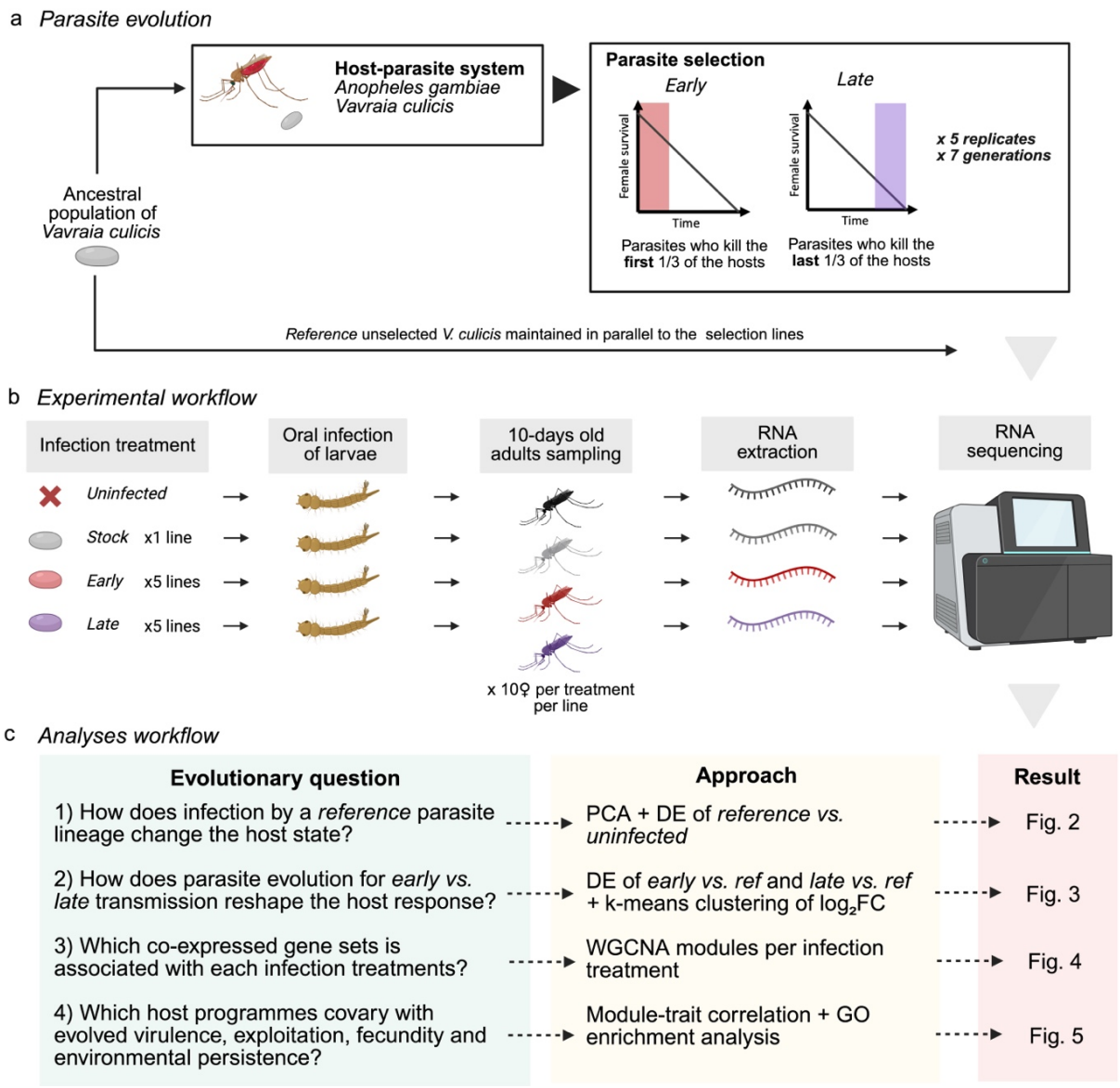

Figure 1. Parasite evolution, experimental and analytical workflow. (a) An ancestral *Vavraia culicis* population infecting *Anopheles gambiae* was split into selection regimes. In the *early* regime, spores were collected from hosts dying in the first third of the survival distribution; in the *late* regime, spores were collected from hosts dying in the last third. Selection was applied for seven generations in five replicate parasite lineages per regime, while an unselected *reference* population was maintained in parallel. **(b)** Larval A. gambiae were orally exposed to either no spores (*uninfected*), the *reference* parasite (1 lineage), or *early* or *late* parasites (5 lineages each). Adult females were sampled at day 10 post-emergence, when infections were chronic and sporulating, and RNA was extracted from four independent pools of 10 females per lineage for RNA sequencing. **(c)** Four main evolutionary questions were addressed using different analytical approaches: the core host response to *reference* infection (PCA and differential expression, **Fig. 2**), divergence in host responses to *early vs. late* parasites (Differentially Expression [DE] and k-means clustering of $\log_2$ fold-changes, **Fig. 3**), co-expressed gene sets associated with infection backgrounds (WGCNA modules, **Fig. 4**), and host programmes covarying with evolved virulence, host exploitation and fecundity, and parsaite environmental persistence (WGCNA module–trait correlations, GO enrichment and hub-gene expression, **Figs. 4–5**).

Materials and Methods

Model system

The Kisumu strain of the mosquito *Anopheles gambiae (s.s.)* was used as host. As parasites, 11 independently maintained lineages of the microsporidian *Vavraia culicis floridensis* [30, 31] were used: one unselected laboratory population (*reference*), five lineages selected for early transmission (*early*) and five selected for late transmission (*late*). *Early* lineages were obtained by repeatedly collecting spores from the earliest dying hosts in each generation, favouring parasites that completed their life cycle rapidly and killed hosts sooner. Late lineages were obtained by collecting spores from the latest dying hosts, favouring parasites that remained longer within the host before transmission [12]. The performance of these lineages and their effects on mosquito life history, virulence and parasite exploitation have been characterized in detail [12, 30, 35, 37, 38]. All experiments were conducted under standard conditions (26 ± 1 °C, 70 ± 5% relative humidity, 12:12 h light-dark cycle).

Infection assay and sample collection

Freshly hatched *An. gambiae* larvae were reared in Petri dishes at a density of 50 larvae in 80 ml of distilled water and fed daily with fish food according to a standard regime [12]. On day 2 of larval development, individuals were exposed to 10,000 *V. culicis* spores per larva from the respective parasite line (*early*, *late* or *reference*); *uninfected* controls were handled identically but received no spores. At pupation, individuals were transferred to tubes containing distilled water and allowed to emerge. Adult females were maintained with constant access to 6% sucrose solution.

Females were sampled on day 10 of adulthood, when previous work on these lines has shown that all infections produce infective spores and that virulence differences among parasite lineages are expressed [12]. On that day, all surviving females were collected and stored at −80 °C until RNA extraction. For RNA sequencing, each parasite lineage (*reference*, five *early* lines and five *late* lines; n = 11) and the *uninfected* control were represented by four independent biological replicates, each consisting of an independent pool of 10 females. Replication, therefore, occurred at two levels: each lineage (and the *uninfected* control) was sampled four times, and the *early* and *late* treatments each comprised five independently evolved parasite lineages.

RNA extraction, library preparation and sequencing

Total RNA was extracted from each pool of 10 females using the RNeasy Universal Plus kit (Qiagen). Adults were homogenized in QIAzol reagent with stainless steel beads, and RNA was eluted in nuclease-free water. RNA concentrations were adjusted before shipment on dry ice to the Genomic

Technologies Facility at the University of Lausanne (Switzerland). RNA quality was assessed on a Fragment Analyzer. Libraries were prepared from 250 ng total RNA per sample using the Illumina Stranded mRNA Prep kit with unique dual indices, quantified and checked for size distribution, and sequenced as single-end 150-bp reads on an Illumina NovaSeq 6000 platform, yielding approximately 20–38 million reads per sample after demultiplexing.

Read processing and gene quantification

Adapters and low-quality bases were removed with Cutadapt, and short reads (< 40 nt) were discarded. Reads mapping to rRNA were removed with fastq_screen. Filtered reads were aligned against a concatenated reference combining the *An. gambiae* genome (assembly GCA_943734735.2) and the *V. culicis floridensis* genome (GCA_000192795.1) using STAR. Gene-level counts were obtained with htseq-count using the corresponding GTF annotation files. Alignment quality was assessed with RSeQC; libraries showed high alignment rates to the mosquito genome with broad coverage across expressed genes. Analyses focus on host (*An. gambiae*) gene expression; parasite reads were retained during alignment but were not analyzed further here **(File S1, Table S1, Figure S1)**.

Expression filtering and normalization

Bioinformatic processing and downstream analyses were conducted in R (version 4.3.1). Gene-level count tables were filtered to remove lowly expressed genes, retaining genes that reached a minimum counts-per-million threshold in a minimum number of libraries. Library sizes were normalized using the trimmed mean of M-values (TMM) method, and $\log_2$-counts-per-million (logCPM) values were used for exploratory analyses and linear modelling. For multivariate and network analyses, variance-stabilized expression measures derived from the normalized counts were used where appropriate. The normalized expression matrix was saved as a genes × samples table and imported into R for the statistical analyses described below.

Statistical analyses

Analyses and plotting were performed in R 4.3.1 using standard tidyverse packages [39], as well as clusterProfiler [40] and WGCNA [41]. Analyses were structured to (i) quantify a core infection signature by comparing *reference* infections with *uninfected* controls; (ii) quantify divergence in host expression between *early* and *late* infections relative to the *reference*; and (iii) identify co-expression modules and relate them to independent measurements of parasite life-history traits (virulence, host exploitation, fecundity and environmental persistence) obtained from the same evolved lines.

190 For principal component analysis (PCA), the upper 75% most variable genes were retained, and PCA
191 was performed on the transposed, centred and scaled expression matrix using prcomp [42]. Differential
192 expression between treatments was assessed using gene-wise two-sample t-tests on $\log_2$-transformed,
193 normalized expression values, with p-values adjusted using the Benjamini–Hochberg correction. Unless
194 stated otherwise, genes with a false discovery rate (FDR) < 0.05 and an absolute $\log_2$ fold-change > 2
195 were considered differentially expressed; a slightly more permissive threshold (FDR < 0.05; $|\log_2$ fold-
196 change$| > 1$) was used for overlap and clustering analyses.

197 To analyze patterns across infection treatments, $\log_2$ fold-changes from the three contrasts (*reference*
198 *vs. uninfected*, *early vs. reference*, *late vs. reference*) were combined. Genes that were differentially
199 expressed in at least one contrast were retained, and k-means clustering ($k = 6$) was applied to their $\log_2$
200 fold-change profiles to group genes with similar reaction norms. Weighted gene co-expression network
201 analysis (WGCNA) was used to identify modules of co-regulated genes and relate them to infection
202 treatment and evolved life-history traits. A signed network was constructed from variance-filtered,
203 normalized expression values, and modules were defined using dynamic tree cutting. Module
204 eigengenes were correlated with binary indicators for each infection treatment and with line-level trait
205 means for virulence, host exploitation, fecundity and environmental persistence. Gene Ontology (GO)
206 enrichment for module subsets associated with early and late infections was tested using enrichGO with
207 the "org.Ag.eg.db" annotation[43], defining the expressed gene set as the background. Within the
208 WGCNA network, intramodular connectivity (kME) was used to identify hub genes in modules linked
209 to virulence (M3) and environmental persistence (M9). Gene annotations were obtained from
210 VectorBase and OrthoMCL-DB [44, 45]. A full description of materials and methods can be found in
211 **File S1**.

212

213 **Results**

214 Mosquito transcriptomes were compared across infections with experimentally evolved microsporidian
215 parasites to test how infection strategies remodel the host response and how these changes relate to
216 virulence and other life-history traits. A single *An. gambiae* (Kisumu) background was either left
217 *uninfected*, infected with a *reference V. culicis* population, or infected with parasite lines that had been
218 experimentally evolved for contrasting transmission times [26,27] **(Fig. 1a)**. *Early* lines had been
219 selected to transmit by killing hosts sooner, whereas *late* lines had been selected to transmit after longer
220 within-host persistence [12, 36]. Five independently evolved parasite lineages were available within
221 each of the *early* and *late* regimes, providing replication for evolutionary inferences. In contrast, a single
222 *reference* and a single *uninfected* lineage served as physiological anchors **(Fig. 1b, c)**.

223 Larval mosquitoes were exposed to the different parasite lineages, and adult females were sampled at a
224 common time point, when infections were mature, and previous work on the same lines had

225 demonstrated clear differences in virulence, host exploitation, within-host parasite growth, fecundity,
226 and environmental persistence [12, 35, 36]. RNA was extracted from pools of ten females per sample.
227 Each lineage (and the *uninfected* control) was represented by four replicate pools, yielding 44
228 transcriptomes spanning infection treatments and selection regimes.

229 Across the twelve lineages (one *uninfected*, one *reference*, five *early*, five *late*), 20–38 million reads
230 were obtained per sample, covering over 9,900 genes **(File S1, Table S1 and Fig. S1)**. Reads aligned
231 successfully to the *An. gambiae* genome, and standard quality checks confirmed that libraries and
232 mapping were suitable for downstream analyses **(File S1, Fig. S2 and S3)**.

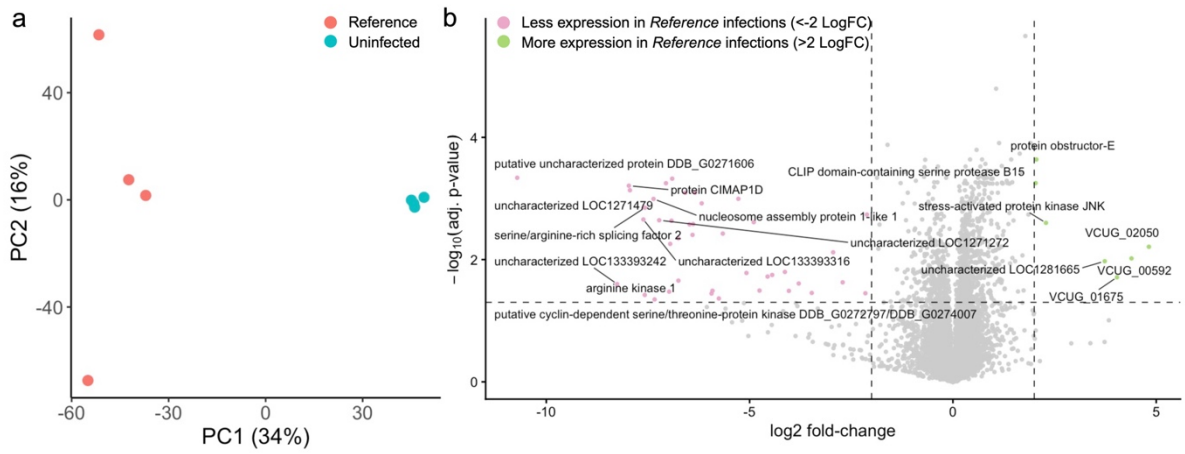

233

234 **Figure 2. Host transcriptional response to a *Reference* infection. (a)** Principal component analysis
235 (PCA) of normalized gene expression in mosquitoes exposed to the *reference V. culicis* line (*reference*,
236 red) or left *uninfected* (*uninfected*, blue). Each point represents one pool of ten females (four
237 independent replicate pools per treatment). PCA was performed on the centred and scaled expression
238 matrix after retaining the 75% most variable genes. The axes show the percentage of variance explained
239 by PC1 and PC2. *Reference* infections separated clearly from *uninfected* controls along PC1, indicating
240 a strong and consistent infection signature. **(b)** Volcano plot of gene expression differences between
241 *reference* and *uninfected* treatments. For each gene, the $\log_2$ fold-change (*reference* - *uninfected*) and
242 the $-\log_{10}$ of the Benjamini–Hochberg adjusted *p*-value are shown. Genes with FDR < 0.05 and $|\log_2 FC|$
243 > 2 are coloured according to whether they show lower (pink) or higher (green) expression in *Reference*
244 infections. The genes with a larger effect size in each direction are labelled.

245

246 *Core response to infection*

247 The *reference* infection induced a strong and coherent shift in mosquito gene expression relative to
248 *uninfected* controls. In a PCA restricted to *reference* and *uninfected* samples, PC1 explained a
249 significant proportion of the variance and separated samples almost entirely by infection status **(Fig.**
250 **2a; File S1, Table S2)**. Variation among replicate pools within each treatment (PC2) was modest
251 compared with the separation between infected and uninfected groups.

Differential expression (DE) analysis between *reference* and *uninfected* treatments confirmed that infection altered the expression of many genes **(Fig. 2b)**. Hundreds of genes showed significant differences (false discovery rate, FDR < 0.05; $|\log_2$ fold change$| > 2$), with both strongly up-regulated and down-regulated loci. Up-regulated genes included several known or putative immune effectors and stress response genes, consistent with activation of canonical defence pathways. Down-regulated genes were enriched for more general metabolic and homeostatic functions, suggesting that infection also involves a reorganization of baseline physiology. This core infection signature was therefore used as a reference state against which evolved parasite infections were compared.

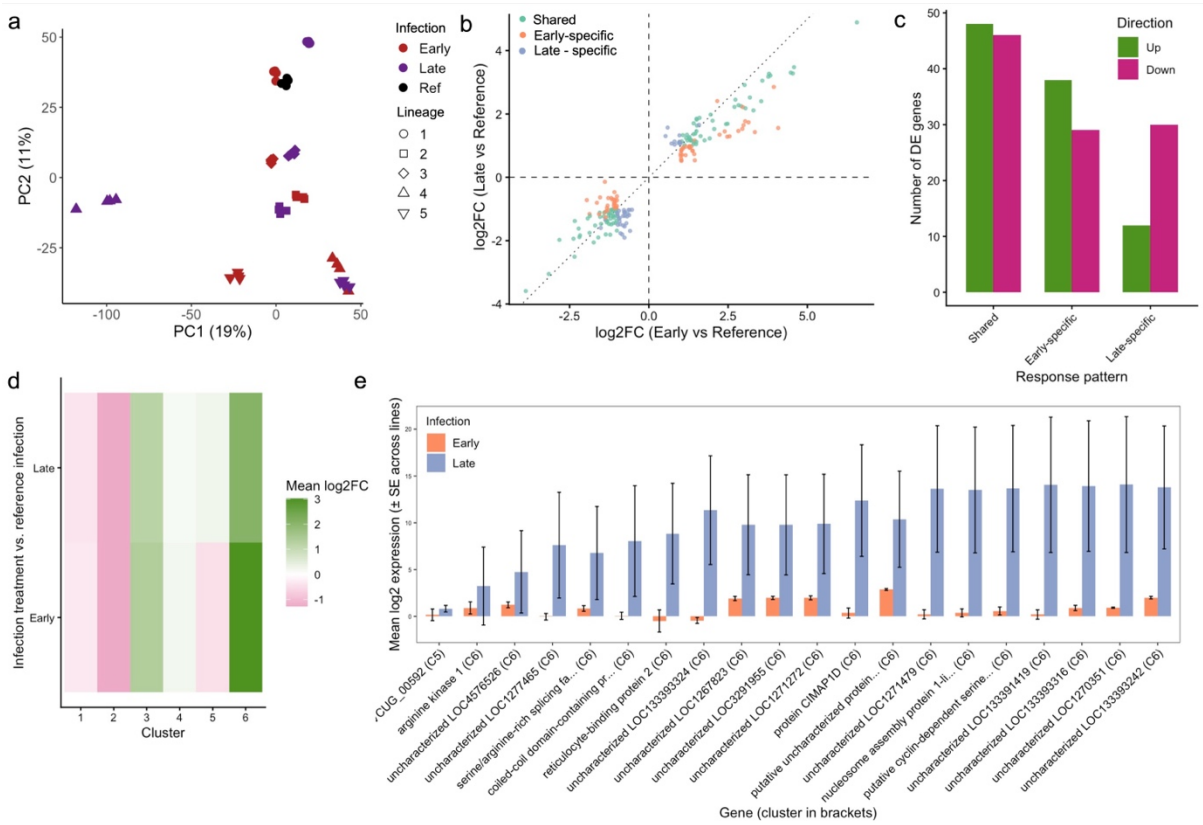

Figure 3. Parasite evolution reshapes the mosquito infection response. (a) PCA of infected treatments only, comparing mosquitoes infected with *reference* (**black**), *early* (**purple**) or *late* (**red**) parasite lineages. Each point represents one pool of ten females. Different symbols indicate the five independently evolved parasite lineages within the *early* and *late* treatments. PCA was performed on the 75% most variable genes across infected samples. *Early* and *late* infections both diverged from the *reference* response, but did so in different regions of PC space. **(b)** Comparison of $\log_2$ fold-changes for *early vs. reference* (x-axis) and *late vs. reference* (y-axis). Each point represents one gene. Genes that were differentially expressed (FDR < 0.05 and $|\log_2 FC| > 1$) in both contrasts with the same sign are shown as shared (**green**), whereas genes that were differentially expressed only in *early* (**orange**) or only in *late* (**blue**) are shown as treatment-specific. Dashed lines indicate zero $\log_2$FC, and the dotted diagonal indicates equal responses in *early* and *late*. **(c)** Numbers of up-regulated (**green**) and down-regulated (**pink**) genes in each response category from panel (b): shared, *early*-specific and *late*-specific.**(d)** k-means clustering of genes that were DE in at least one comparison involving *reference* infections (*reference vs. uninfected*, *early vs. reference*, late *vs*. *reference*). Clustering was performed

on triplets of $\log_2$FC values (missing values set to zero), with k = 6 clusters. The heatmap shows mean $\log_2$FC for *early vs. reference* and *late vs. reference* within each cluster, highlighting groups of genes that respond more strongly in *early* or *late* infections. **(e)** Mean $\log_2$ expression (± SE across lines) of a subset of genes belonging to clusters 5 and 6, which showed particularly strong divergence between *early* and *late* infections. Expression was averaged across replicate pools within each parasite lineage and then across the five *early* or five *late* lineages.

Evolved parasite strategies differentially modify the core response

When only infected samples (*reference*, *early,* and *late*) were considered, the PCA revealed that evolved infections diverged both from the *reference* response and from one another **(Fig. 3a; File S1, Table S3 and Fig. S4)**. Samples clustered primarily by infection regime, with *early* and *late* infections occupying distinct regions of PC space. Replicate lines within each regime tended to cluster together, indicating that experimental evolution produced repeatable shifts in the host transcriptome across independently evolved parasite lineages.

Pairwise differential expression analyses against the *reference* infection showed that both *early* and *late* infections modified the *reference* response, but in partially overlapping and partially distinct ways **(Fig. 3b,c; File S3)**. Genes were classified into response categories based on whether they were differentially expressed (FDR < 0.05; $|\log_2\text{FC}| > 1$) in *early vs. reference*, in *late vs. reference*, in both contrasts in the same direction, or in neither. A substantial set of genes responded in the same direction in both *early* and *late* infections relative to the *reference*, indicating that some aspects of the evolved responses remain conserved across infection strategies. However, sizeable sets of genes were *early*- and *late*-specific, changing expression only in one regime **(Fig. 3c)**. These patterns show that parasite evolution generated distinct infection-specific transcriptomic shifts on top of the shared core response.

To summarise patterns across comparisons, genes that were differentially expressed in at least one of the three infection contrasts (*reference vs. uninfected*, *early vs. reference*, *late vs. reference*) were clustered by their $\log_2$ fold-change profiles. Six k-means clusters captured distinct trajectories of how gene expression changed across the infection sequence **(Fig. 3d; File S4)**. Some clusters consisted of genes strongly induced by the reference infection and further upregulated in *early* infections but attenuated in *late* infections, whereas other clusters showed the opposite pattern, with expression enhanced in *late* infections. Examination of representative genes from the most divergent clusters highlighted genes whose mean expression differed consistently between *early* and *late* infections across replicate lines **(Fig. 3e)**. Together, these analyses show that parasite infection strategies have remodelled the host transcriptome in repeatable but regime-specific ways.

Co-expression modules link infection backgrounds to eco-evolutionary traits

WGCNA was used to group genes into modules that co-varied across all transcriptomes and to relate these modules to infection backgrounds and independently measured life history traits. Seventeen modules (M0–M16) were detected. Correlations between module eigengenes and infection treatments showed that several modules tracked specific infection backgrounds **(Fig. 4a; File S5 and S6)**. Modules M14, M15, M6 and M9 were positively associated with *early* infections. In contrast, modules M0 and M16 were positively associated with *late* infections. These modules, therefore, capture gene programmes that differ across parasite infection strategies within the shared mosquito background.

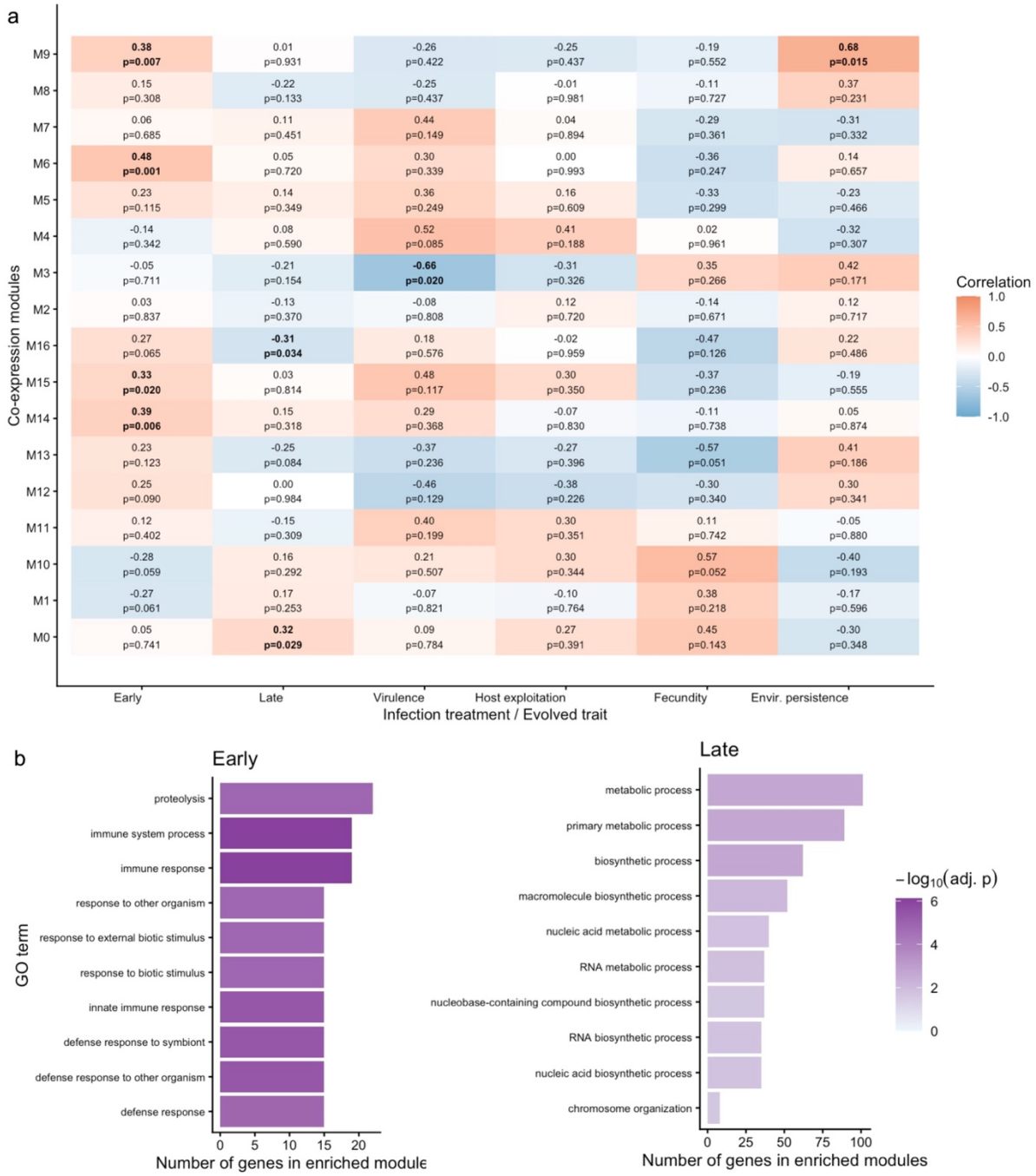

Figure 4. Co-expression modules connect evolved parasites with immune and metabolic gene programmes. (a) Correlations between module eigengenes and infection backgrounds or evolved life-

history traits. Rows correspond to WGCNA modules (M0–M16). Columns correspond to infection treatments by evolved parasites (*early* or *late*) or line-level traits: virulence (maximum mortality hazard), host exploitation (spore density at day 10), fecundity at day 10, and environmental persistence (infection probability after 90 days outside the host). Each tile shows the Pearson correlation coefficient (colour scale) and the associated *p*-value; significant associations ($p < 0.05$) are indicated in bold. Modules M14, M15, M6 and M9 showed positive associations with *early* infections, whereas M0 and M16 were positively associated with *late* infections. Module M3 was negatively correlated with virulence, and module M9 was positively correlated with environmental persistence. **(b)** Gene Ontology (GO) enrichment of modules linked to *early* and *late* infections. Modules most strongly associated with *early* infections (M14, M15, M6 and M9; left panel) or *late* infections (M0 and M16; right panel) were grouped, and GO Biological Process enrichment was tested relative to the expressed gene universe. Bars show the number of genes in the enriched module set that mapped to each GO term, ordered by gene count. Bar colour intensity represents $-\log_{10}$ of the adjusted *p*-value. *Early*-biased modules were enriched for immune and defence processes, whereas *late*-biased modules were enriched for RNA metabolic and core biosynthetic processes.

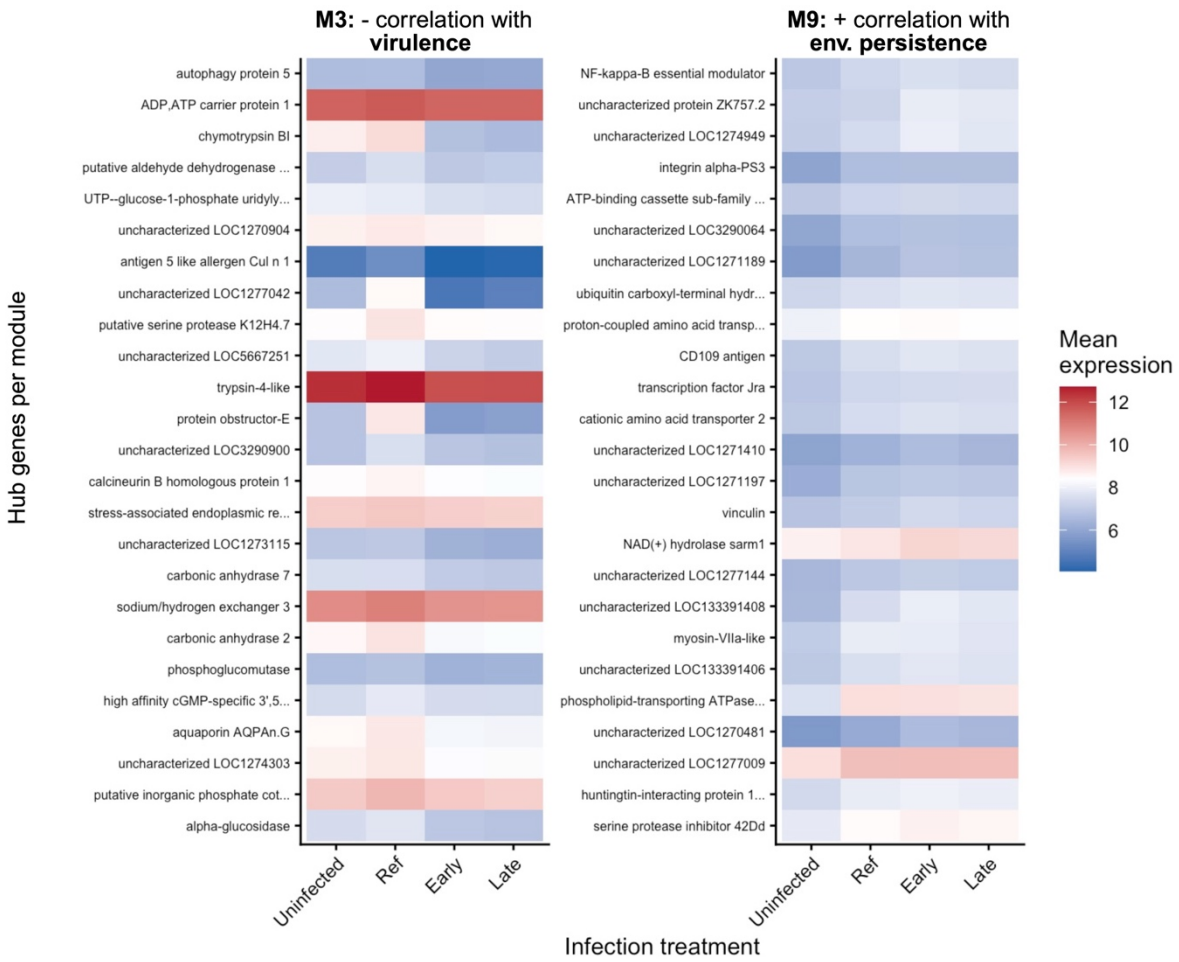

Figure 5. Hub genes in virulence- and environmental persistence-associated modules show distinct expression profiles across infection regimes. Heatmaps of mean expression for the top 25 hub genes (highest intramodular connectivity, kME) in module M3 (left) and module M9 (right). Module M3 showed a negative correlation with virulence, whereas module M9 showed a positive

correlation with environmental persistence (Fig. 4a). Rows correspond to individual hub genes, ordered within each module by decreasing |kME|. Columns correspond to infection treatments: *uninfected*, *reference*, *early* and *late*. For each gene × treatment combination, normalized expression values were transformed to $\log_2(\text{count} + 1)$ and averaged across all replicate samples belonging to that treatment. Colour scale indicates mean expression, with red tones denoting higher expression and blue tones denoting lower expression. Together, these patterns highlight candidate genes whose expression shifts across infection regimes may mediate the trade-off between virulence and environmental survival of the parasite.

The same modules were then related to virulence, host exploitation, fecundity and parasite environmental persistence, previously measured in the same evolved lines [12, 36]. Module M3 was negatively correlated with virulence, such that linages with higher M3 expression tended to exhibit lower mortality hazards. In contrast, module M9 was positively correlated with environmental persistence, indicating that higher expression of this module tended to occur in parasite lines whose spores remained infective for longer outside the host. Modules associated with *early* or *late* infections showed weaker or more trait-specific correlations, suggesting that only a subset of infection-linked programmes is tightly aligned with the measured life history outcomes.

Functional enrichment of infection-linked modules supported a division between immune and metabolic programmes. *Early*-associated modules (M14, M15, M6, and M9) were enriched for immune- and defence-related Gene Ontology (GO) terms, including responses to pathogens, proteolysis, and signalling processes **(Fig. 4b; File S7)**. In contrast, late-associated modules (M0 and M16) were enriched for RNA metabolic processes and core biosynthetic functions. These results indicate that parasite infection strategies have partitioned the host transcriptome into immune-biased and metabolically biased programmes that align with experimentally evolved infection regimes.

Hub genes associated with virulence and environmental persistence

To identify candidate genes most strongly linked to the eco-evolutionary outcomes, intramodular connectivity (kME) was used to rank genes within each module. Modules that showed clear associations with virulence and environmental persistence were examined in more detail. In module M3, which was negatively correlated with virulence, the 25 genes with the highest kME values were selected as hub genes. A similar set of 25 hub genes was selected from module M9, which was positively correlated with environmental persistence.

Heatmaps of mean expression of these hub genes across the four infection treatments showed distinct patterns for M3 and M9 **(Fig. 5; File S8).** Many M3 hub genes displayed relatively low expression in *uninfected* mosquitoes, increased expression in the *reference* infection, and further changes in *early* and *late* infections consistent with the negative association between this module and virulence. By contrast,

377 M9 hub genes tended to show expression patterns that matched the positive association with
378 environmental persistence, with characteristic differences between *early* and *late* infections. Several
379 hub genes in both modules had immune or metabolic annotations, reinforcing the idea that immune and
380 metabolic programmes are key axes along which infection strategies, virulence and persistence are
381 linked.

382

383 **Discussion**

384 Parasites have a diverse array of strategies and life histories, many of which are constrained by their
385 ecology and by trade-offs between within-host performance and between-host survival. Evolutionary
386 theory predicts that these differences in parasite strategy should be expressed through the host, as
387 variation in exploitation, per-parasite pathogenicity, resistance, and tolerance jointly determines
388 virulence [2, 11, 22]. In this system, lineages of the microsporidian *V. culicis* have been selected for
389 earlier or later transmission, generating parasite populations that differ in growth, virulence and
390 environmental persistence while sharing the same *An. gambiae* host background. Previous work on
391 these lineages has shown that *late*-selected parasites grow faster, reach higher spore loads, are more
392 virulent, and reduce the environmental persistence of spores, whereas *early*-selected lines are less
393 virulent, exploit hosts less intensely, and maintain infectivity longer outside the host [12, 35, 36]. The
394 present study adds a transcriptomic layer at a single, common time point (day 10 of adulthood) to ask
395 how these evolved parasite life histories influence host gene expression and how host co-expression
396 modules covary with virulence, host exploitation, fecundity, and environmental persistence **(Fig. 1)**.

397

398 *A conserved core response to infection provides the baseline*

399 The comparison between *uninfected* and *reference*-infected mosquitoes revealed a strong and consistent
400 infection signature **(Fig. 2)**. Samples separated clearly in multivariate space, and hundreds of genes
401 were differentially expressed. Previous work showed that reference infections already impose
402 detectable costs on survival and fecundity by day 10 [12]. The core transcriptional response observed
403 here at the same time point likely reflects parasite recognition, canonical immune effectors (including
404 melanization, antimicrobial peptides, and cellular responses), and systemic adjustments in metabolism
405 and stress management needed to support both the host and the parasite.

406 When this response is compared with an earlier study using *V. culicis* in *Aedes aegypti*, more genes and
407 larger expression changes were reported in *Aedes* than in *Anopheles* [46]. If these additional genes
408 enhance immunity, they may help explain the higher survival and resistance of *Aedes* relative to
409 *Anopheles* against the same generalist parasite [31]. In other words, *V. culicis* elicits a robust but host-
410 specific programme, and the *Anopheles* response appears more constrained. This *reference* response in

411 *An. gambiae* provides a valuable baseline against which divergence in host responses due to parasite
412 life-history evolution can be interpreted.

413

414 *Divergent host response under early and late infection*

415 When only infected treatments were considered, *early*, *late* and *reference* infections occupied
416 overlapping but distinct regions of transcriptomic space **(Fig. 3a)**. All infections shared the core
417 response, consistent with the fact that by day 10, all lines had completed their life cycle and were
418 producing spores [12]. However, pairwise comparisons against the reference revealed a mixture of
419 shared and regime-specific changes. Many genes were differentially expressed in both *early* and *late*
420 infections in the same direction, whereas others changed only in *early* or only in *late* lines **(Fig. 3b,c)**.

421 Clustering $\log_2$ fold-changes across *reference vs. uninfected*, *early vs. reference* and *late vs. reference*
422 summarised these patterns into a small number of reaction-norm profiles **(Fig. 3d)**. Some clusters
423 represented a generic infection response that was further amplified by both evolved regimes. Others
424 captured genes whose expression differed between *early* and *late* infections at the same time point **(Fig.
425 3e)**. Because all measurements were taken on day 10, these differences reflect distinct host–parasite
426 states under different parasite strategies, rather than differences in infection age.

427 These patterns are consistent with the broader life-history phenotyping. *Late* parasites grow faster, reach
428 higher chronic loads, cause higher adult mortality and induce earlier reproduction and shifts in resource
429 allocation than early parasites [12, 35, 36]. The fact that distinct gene clusters separate *early* and *late*
430 infections suggests that hosts are in measurably different physiological states by day 10, depending on
431 the parasite strategy they carry, even though the basic infection cycle is shared.

432

433 *Co-expression modules link infection backgrounds to host response space*

434 The co-expression network analysis provides a more integrated view of these differences **(Fig. 4)**.
435 WGCNA grouped genes into modules whose eigengenes varied across *uninfected*, *reference*, *early* and
436 *late* infection treatments. Some modules behaved as general infection modules, with elevated
437 eigengenes in all infected treatments relative to *uninfected* controls. Others were more clearly associated
438 with *early* or *late* infections, indicating that experimental evolution has altered how specific gene
439 networks are regulated.

440 Modules most strongly associated with early infections (M14, M15, M6, and M9) were enriched for
441 immune, defence, and stress-related GO terms, as well as transcriptional and regulatory processes. In
442 contrast, modules associated with late infections (M0 and M16) were enriched for RNA metabolism,
443 biosynthesis and broader metabolic functions. Although GO categories are coarse, this separation

suggests that *early* and *late* parasite regimes push the host into different regions of response space. *Early* parasites, which are less virulent and reach lower chronic loads, are likely still constrained by classical immune and stress responses reflected in these modules. For *late* parasites, which are more virulent and reach higher loads, immune-annotated modules are less prominent; instead, transcriptional and metabolic rewiring dominate.

Several non-exclusive mechanisms could underlie this pattern. *Late* parasites may reduce early immune recognition or dampen effector deployment [47–49], allowing faster growth despite a comparatively "quieter" immune readout. Hosts may rely more on metabolic reorganization and damage control to maintain key functions at higher parasite burdens, a pattern closer to disease tolerance than to resistance. In addition, independent life-history work showed that *late* infections induce earlier reproduction and a shift away from somatic maintenance, consistent with terminal investment by the host under high mortality risk [27, 28]. Taken together, the module structure suggests that *early* infections are characterized by a stronger immune and stress response, whereas *late* infections are characterized by greater changes in biosynthesis, energy use, and metal handling.

These module-level patterns align closely with previous biochemical and metallomics phenotyping of the same lines. *Late* infections increased protein and carbohydrate reserves and altered metal homeostasis, especially for iron, zinc and manganese, relative to *reference* infections [35]. Modules that are upregulated in *late* infections and enriched for metabolic and metal-related functions, therefore, provide a plausible molecular counterpart to these organismal changes.

A disease tolerance programme associated with lower virulence

A central aim of this study was to connect host expression patterns to the eco-evolutionary outcomes previously quantified in these lines [12, 35, 36] **(Figs. 4 and 5)**. Relating module eigengenes to independent estimates of virulence, host exploitation, fecundity and environmental persistence identified a small number of modules with clear trait associations. Among these, M3 was most strongly and negatively associated with virulence.

Higher M3 eigengene values occurred in infection backgrounds with lower virulence and lower maximum mortality hazard, whereas more virulent backgrounds had lower M3 values at the same stage of infection. The hub genes in M3 pointed to damage limitation and barrier maintenance rather than direct pathogen killing. They included an autophagy protein 5 homologue, an ADP/ATP carrier, digestive serine proteases, obstructor-E, carbonic anhydrases and ion exchangers, consistent with the turnover of damaged components, the stabilization of epithelial surfaces, and the regulation of local pH and ion balance. Uncharacterized loci with informative orthology reinforced this picture: a

478 glucuronosyltransferase-like gene suggests roles in conjugation and detoxification of reactive
479 metabolites; a Niemann–Pick type C-2 orthologue points to lipid trafficking and membrane
480 homeostasis; and a ladinin-1-like gene links to basement-membrane integrity.

481 This combination of functions is easier to interpret as limiting tissue damage and maintaining barrier
482 function than as directly reducing parasite numbers. In other words, higher M3 activity likely reduces
483 the harm caused by infection at a given parasite burden. M3 therefore stands out as a candidate disease
484 tolerance programme in this system [9, 50]: a coordinated set of damage-control and barrier-
485 maintenance genes whose upregulation is associated with lower virulence across evolved lines. Similar
486 tolerance-like modules have been proposed in vertebrate models [51–53] but remain rare in invertebrate
487 systems [4, 8, 54, 55], making M3 a useful starting point for comparative and functional work. Such
488 tolerance-like programmes are predicted to relax selection on parasite load and allow for clonal
489 interference, potentially reshaping the evolutionary routes available to *V. culicis* and other parasites [22,
490 56, 57].

491

492 *A transmission-linked programme associated with environmental persistence*

493 M9, in contrast, aligned most clearly with the environmental-persistence axis **(Figs. 4 and 5)**. Higher
494 M9 eigengene values were observed in backgrounds whose spores maintained infectivity in the
495 environment longer, whereas lower values were observed in lines whose spores lost infectivity more
496 quickly. The hubs in this module pointed to functions that can shape the microenvironment in which
497 spores mature and are released.

498 Key examples include a phosphatase-like gene, a low-density-lipoprotein-receptor-domain-containing
499 gene, phospholipase A2, pleckstrin and a polycystic kidney disease protein 1-like gene, all of which are
500 typically involved in membrane signalling, lipid handling, mechanosensation and cell-surface
501 organization. Additional hubs, such as a POU transcription factor, glycine cleavage H protein,
502 transcriptase-domain-containing proteins and a zinc-finger protein, point to transcriptional and
503 mitochondrial regulation. One of the most connected loci lacks informative annotation but sits centrally
504 in the module, suggesting an as-yet undescribed role in these pathways.

505 Such a collection of hubs is compatible with a module that conditions the chemical and physical
506 environment experienced by spores, for example, by modifying lipid and ion composition in gut and
507 tissue spaces, altering extracellular matrices and cuticular or peritrophic structures where spores
508 accumulate, and controlling vesicle trafficking and secretion around host death. Under this
509 interpretation, M9 represents a host programme that shapes the quality and robustness of transmission
510 stages rather than directly altering within-host damage. This highlights an often overlooked layer of

511 virulence evolution: hosts can shape not only whether parasites transmit, but also the quality and
512 durability of the transmission stages they release into the environment.

513 This interpretation is in line with previous work on the same lineages [35, 36]. In those studies, *early*
514 parasites produced spores that remained infective for longer in water, whereas *late* parasites produced
515 spores that lost infectivity more rapidly [36]. Infection with these lineages also altered mosquito energy
516 stores and the balance of several elements [35], indicating that the physiological environment in which
517 spores are formed depends on the parasite's strategy. In that context, the association of M9 with genes
518 involved in lipid handling, membrane organization, and mitochondrial function suggests that this
519 module captures how the host tunes the environment: by altering membranes, vesicle traffic, and local
520 metabolism in tissues where spores accumulate. Hence, the host effectively sets the conditions for
521 departure that influence how robust and long-lived spores will be once released into aquatic habitats.

522 The opposite associations of M3 and M9 with virulence and environmental persistence mirror the trade-
523 off previously described between within-host performance and environmental survival in these lines
524 [22, 36]: late parasites grow faster and are more virulent but produce spores that lose infectivity quickly,
525 whereas early parasites are less virulent but retain infectivity for longer. The fact that these axes are
526 recapitulated by host modules identified independently from expression structure suggests that a small
527 set of host programmes may play a disproportionate role in how evolved parasite strategies translate
528 into virulence and transmission. This represents a concrete example of how selection on parasite life
529 history can reveal underlying host tolerance and transmission programmes.

530

531 *Conclusions*

532 Overall, this study links experimental evolution, life-history phenotypes and host transcriptomic
533 architecture in a natural mosquito–microsporidian system. It shows that evolved parasite life history is
534 reflected in distinct host expression states, identifies a co-expression module consistent with disease
535 tolerance, and highlights a second module that appears to condition the environment encountered by
536 transmission stages. These results suggest that key associations between virulence, tolerance, host
537 exploitation and environmental persistence can be mapped onto identifiable host modules and hub
538 genes, providing tractable targets for functional work in this and other host–parasite systems.

539 Taken together, these modules have broader implications for microbial ecology, disease ecology and
540 epidemiology. The tolerance-associated M3 module shows that hosts can modulate damage limitation
541 and barrier integrity without necessarily hindering parasite growth. In contrast, the environmental-
542 persistence module M9 suggests that hosts also remodel the environments in which transmission stages
543 develop and are released. Therefore, hosts can act as niche constructors for their parasites: by adjusting
544 tissue integrity, membrane organization, metal and lipid handling, and secretion around host death, they

generate a mosaic of internal and external microhabitats that microbial lineages must withstand or exploit. They thereby directly shape the ecological niches, selective pressures and transmission opportunities that underlie microbial life-history and virulence evolution.

More broadly, the approach used here, *i.e.* evolving parasite life histories and reading out the resulting host programmes, could be applied across vector and non-vector systems to dissect how resistance, tolerance and transmission are genetically implemented in nature. Extending this framework to additional host–parasite combinations and to structured or fluctuating environments should help clarify when and how host niche construction feeds back on parasite evolution and infection dynamics.

Author contributions

LMS designed and conducted the experiments, analyzed the data and wrote the manuscript.

Acknowledgements

I thank Amjad Khalaf, Ian Will, Paula Escuer Pifarré, Thomas J. Travers-Cook and Tiago G. Zeferino for their advice and experimental support. I also thank the Lausanne Genomic Technologies Facility (University of Lausanne, Switzerland) team, including Johann Weber, Julien Marquis, Sandra Calderon Copete, and Viviane Praz, for their assistance with library preparation, sequencing, and preliminary data analyses. I would especially like to thank Jacob C. Koella and Kayla C. King for their constant feedback, support, and critical comments on the first draft of the manuscript. The project was supported by the Basler Stiftung für biologische Forschung and LMS, funded by a SNF grant 310030_192786.

Competing interests

The author declares that they have no competing interests.

Data availability

All data generated or analyzed during this study are included in this published article and its supplementary information files (Files S9-S13).

References

1. Silva LM, King KC. Ecology and evolution of virulence. *Curr Biol* 2025.

575 https://doi.org/http://doi.org/10.1016/j.cub.2025.08.029

576 2. Råberg L, Stjernman M. The evolutionary ecology of infectious disease virulence.
577 *Ecoimmunology* 2012;**548**:78.

578 3. Wollein Waldetoft K, Råberg L, Lood R. Proliferation and benevolence—A framework for
579 dissecting the mechanisms of microbial virulence and health promotion. *Evol Appl*
580 2020;**13**:879–888. https://doi.org/https://doi.org/10.1111/eva.12952

581 4. Macedo da Silva LM. Pathogen infection dynamics and the evolution of host resistance and
582 tolerance. 2021. 2021.

583 5. Akyaw PA et al. Pathogen-induced damage in Drosophila: uncoupling disease tolerance from
584 resistance. *PLoS Pathog* 2025;**21**:e1013482.

585 6. Medzhitov R, Schneider DS, Soares MP. Disease tolerance as a defense strategy. *Science (80-)*
586 2012;**335**:936–941.

587 7. McCarville JL, Ayres JS. Disease tolerance: concept and mechanisms. *Curr Opin Immunol*
588 2018;**50**:88–93.

589 8. Silva RCMC et al. Heme oxygenase-1 in protozoan infections: A tale of resistance and disease
590 tolerance. *PLoS Pathog* 2020;**16**:e1008599.

591 9. Soares MP, Teixeira L, Moita LF. Disease tolerance and immunity in host protection against
592 infection. *Nat Rev Immunol* 2017;**17**:83.

593 10. Martins R et al. Disease tolerance as an inherent component of immunity. *Annu Rev Immunol*
594 2019;**37**:405–437.

595 11. Acuña-Hidalgo B et al. Decomposing virulence to understand bacterial clearance in persistent
596 infections. *Nat Commun* 2022;**13**:1–14. https://doi.org/https://doi.org/10.1038/s41467-022-
597 32118-1

598 12. Silva LM, Koella JC. Complex interactions in the life cycle of a simple parasite shape the
599 evolution of virulence. *PLoS Pathog* 2025.
600 https://doi.org/https://doi.org/10.1371/journal.ppat.1013294

601 13. Anderson RM, May RM. Coevolution of hosts and parasites. *Parasitology* 1982;**85**:411–426.
602 https://doi.org/https://doi.org/10.1017/S0031182000055360

603 14. May RM, Anderson RM. Epidemiology and genetics in the coevolution of parasites and hosts.
604 *Proc R Soc London Ser B Biol Sci* 1983;**219**:281–313.
605 https://doi.org/https://doi.org/10.1098/rspb.1983.0075

15. Alizon S et al. Virulence evolution and the trade-off hypothesis: history, current state of affairs and the future. *J Evol Biol* 2009;**22**:245–259. https://doi.org/https://doi.org/10.1111/j.1420-9101.2008.01658.x

16. Kun Á et al. Do pathogens always evolve to be less virulent? The virulence–transmission trade-off in light of the COVID-19 pandemic. *Biol Futur* 2023;**74**:69–80.

17. Acevedo MA et al. Virulence-driven trade-offs in disease transmission: A meta-analysis. *Evolution (N Y)* 2019;**73**:636–647.

18. Ben-Ami F. The virulence–transmission relationship in an obligate killer holds under diverse epidemiological and ecological conditions, but where is the tradeoff? *Ecol Evol* 2017;**7**:11157–11166. https://doi.org/https://doi.org/10.1002/ece3.3532

19. Ebert D, Weisser WW. Optimal killing for obligate killers: the evolution of life histories and virulence of semelparous parasites. *Proc R Soc London Ser B Biol Sci* 1997;**264**:985–991. https://doi.org/https://doi.org/10.1098/rspb.1997.0136

20. Breban R. Role of environmental persistence in pathogen transmission: a mathematical modeling approach. *J Math Biol* 2013;**66**:535–546.

21. VanderWaal KL, Ezenwa VO. Heterogeneity in pathogen transmission. *Funct Ecol* 2016;**30**:1606–1622.

22. Silva LM, King KC, Koella JC. Dissecting transmission to understand parasite evolution. *PLoS Pathog* 2025;**21**:e1012964. https://doi.org/https://doi.org/10.1371/journal.ppat.1012964

23. Wolinska J, King KC. Environment can alter selection in host–parasite interactions. *Trends Parasitol* 2009;**25**:236–244.

24. Stearns SC. Trade-offs in life-history evolution. *Funct Ecol* 1989;**3**:259–268. https://doi.org/https://doi.org/10.2307/2389364

25. Agnew P, Koella JC, Michalakis Y. Host life history responses to parasitism. *Microbes Infect* 2000;**2**:891–896.

26. Koella JC, Agnew P %J J of EB. A correlated response of a parasite's virulence and life cycle to selection on its host's life history. 1999;**12**:70–79.

27. Duffield KR et al. A dynamic threshold model for terminal investment. *Behav Ecol Sociobiol* 2017;**71**:1–17.

28. Clutton-Brock TH. Reproductive effort and terminal investment in iteroparous animals. *Am Nat* 1984;**123**:212–229.

637 29. Hudson AL, Moatt JP, Vale PF. Terminal investment strategies following infection are
638 dependent on diet. *J Evol Biol* 2020;**33**:309–317.

639 30. Silva LM, Zeferino TG, Koella JC. Vavraia culicis. *Trends Parasitol* 2025.
640 https://doi.org/https://doi.org/10.1016/j.pt.2025.02.011

641 31. Zeferino TG, Koella JC. Host-specific effects of a generalist parasite of mosquitoes. *Sci Rep*
642 2024;**14**:18365. https://doi.org/https://doi.org/10.1038/s41598-024-69475-4

643 32. Fraiture M et al. Two mosquito LRR proteins function as complement control factors in the
644 TEP1-mediated killing of Plasmodium. *Cell Host Microbe* 2009;**5**:273–284.

645 33. Kramer LD, Ciota AT. Dissecting vectorial capacity for mosquito-borne viruses. *Curr Opin*
646 *Virol* 2015;**15**:112–118.

647 34. Black IV WC et al. Flavivirus susceptibility in Aedes aegypti. *Arch Med Res* 2002;**33**:379–388.

648 35. Silva LM, Vallat A, Koella JC. Mechanisms of host exploitation by a microsporidian parasite.
649 *Proc R Soc B* 2025. https://doi.org/https://doi.org/10.1098/rspb.2025.1123

650 36. Silva LM, Koella JC. Virulence evolution: thinking outside of the host. *Evol Appl*
651 2025;**18**:e70136.

652 37. Penczykowski RM, Laine A, Koskella B. Understanding the ecology and evolution of host–
653 parasite interactions across scales. *Evol Appl* 2016;**9**:37–52.

654 38. Zeferino TG, Silva LM, Koella JC. Energetic shifts reflect survival likelihood in Anopheles
655 gambiae. *Commun Biol* 2025;**8**:1558.

656 39. Wickham H, Wickham MH. Package tidyverse. *Easily Install load 'Tidyverse* 2017.

657 40. Yu G et al. clusterProfiler: an R package for comparing biological themes among gene clusters.
658 *Omi a J Integr Biol* 2012;**16**:284–287.

659 41. Langfelder P, Horvath S. WGCNA: an R package for weighted correlation network analysis.
660 *BMC Bioinformatics* 2008;**9**:559.

661 42. Hothorn T et al. Package 'multcomp'. *Simultaneous inference Gen Parametr Model Proj Stat*
662 *Comput Vienna, Austria* 2016.
663 https://doi.org/https://doi.org/10.32614/CRAN.package.multcomp

664 43. Carlson M. Genome wide annotation for Anopheles, primarily based on mapping using Entrez
665 Gene identifiers.

666 44. Lawson D et al. VectorBase: a data resource for invertebrate vector genomics. *Nucleic Acids*

667 *Res* 2009;**37**:D583–D587.

668 45. Chen F et al. OrthoMCL-DB: querying a comprehensive multi-species collection of ortholog
669 groups. *Nucleic Acids Res* 2006;**34**:D363–D368.

670 46. Desjardins CA et al. Contrasting host–pathogen interactions and genome evolution in two
671 generalist and specialist microsporidian pathogens of mosquitoes. *Nat Commun* 2015;**6**:7121.
672 https://doi.org/https://doi.org/10.1038/ncomms8121

673 47. Koella JC, Boëte C. A model for the coevolution of immunity and immune evasion in vector-
674 borne diseases with implications for the epidemiology of malaria. *Am Nat* 2003;**161**:698–707.

675 48. Foster TJ. Immune evasion by staphylococci. *Nat Rev Microbiol* 2005;**3**:948–958.

676 49. Kim HK et al. Recurrent infections and immune evasion strategies of Staphylococcus aureus.
677 *Curr Opin Microbiol* 2012;**15**:92–99.

678 50. Richardson LA. Understanding disease tolerance and resilience. *PLoS Biol* 2016;**14**:e1002513.

679 51. Råberg L, Sim D, Read AF. Disentangling genetic variation for resistance and tolerance to
680 infectious diseases in animals. *Science (80-)* 2007;**318**:812–814.
681 https://doi.org/https://doi.org/10.1126/science.114852

682 52. Ayres JS, Schneider DS. Tolerance of infections. *Annu Rev Immunol* 2012;**30**:271–294.

683 53. Kellum JA et al. Understanding the inflammatory cytokine response in pneumonia and sepsis:
684 results of the Genetic and Inflammatory Markers of Sepsis (GenIMS) Study. *Arch Intern Med*
685 2007;**167**:1655–1663.

686 54. Troha K et al. Comparative transcriptomics reveals CrebA as a novel regulator of infection
687 tolerance in D. melanogaster. *PLoS Pathog* 2018;**14**:e1006847.

688 55. Howick VM, Lazzaro BP. Genotype and diet shape resistance and tolerance across distinct
689 phases of bacterial infection. *BMC Evol Biol* 2014;**14**:56.

690 56. Miller MR, White A, Boots M. The evolution of parasites in response to tolerance in their hosts:
691 the good, the bad, and apparent commensalism. *Evolution (N Y)* 2006;**60**:945–956.

692 57. Strelkowa N, Lässig M. Clonal interference in the evolution of influenza. *Genetics*
693 2012;**192**:671–682. https://doi.org/https://doi.org/10.1534/genetics.112.143396

694

a *Parasite evolution*

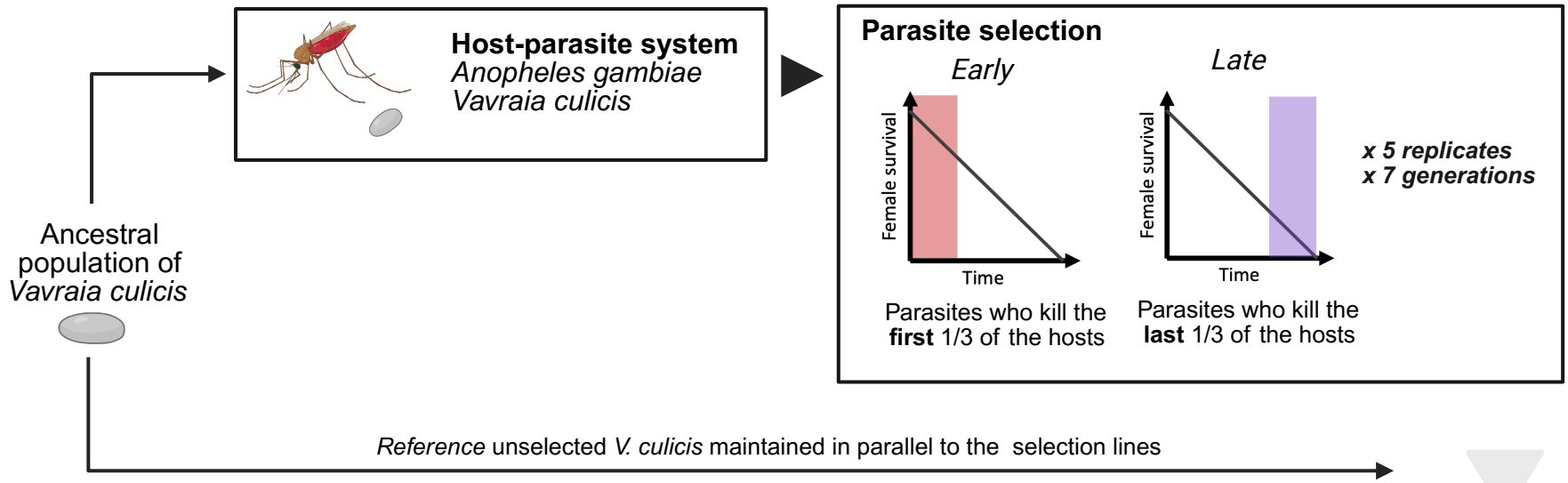

b *Experimental workflow*

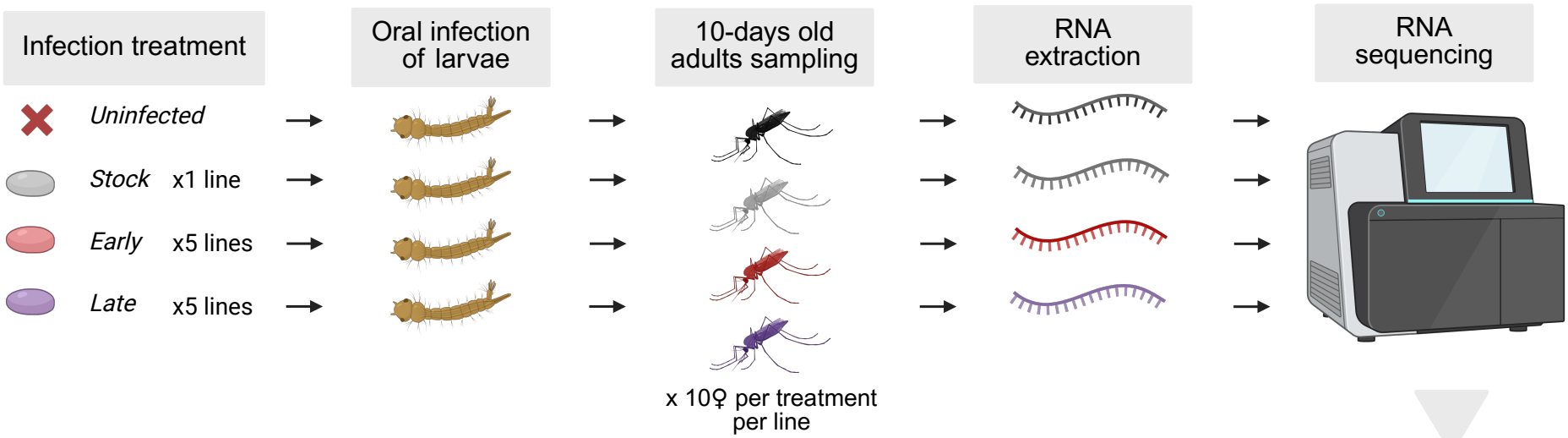

c *Analyses workflow*

Evolutionary question	Approach	Result
1) How does infection by a *reference* parasite lineage change the host state?	PCA + DE of *reference vs. uninfected*	Fig. 2
2) How does parasite evolution for *early vs. late* transmission reshape the host response?	DE of *early vs. ref* and *late vs. ref* + k-means clustering of log_2FC	Fig. 3
3) Which co-expressed gene sets is associated with each infection treatments?	WGCNA modules per infection treatment	Fig. 4
4) Which host programmes covary with evolved virulence, exploitation, fecundity and environmental persistence?	Module-trait correlation + GO enrichment analysis	Fig. 5

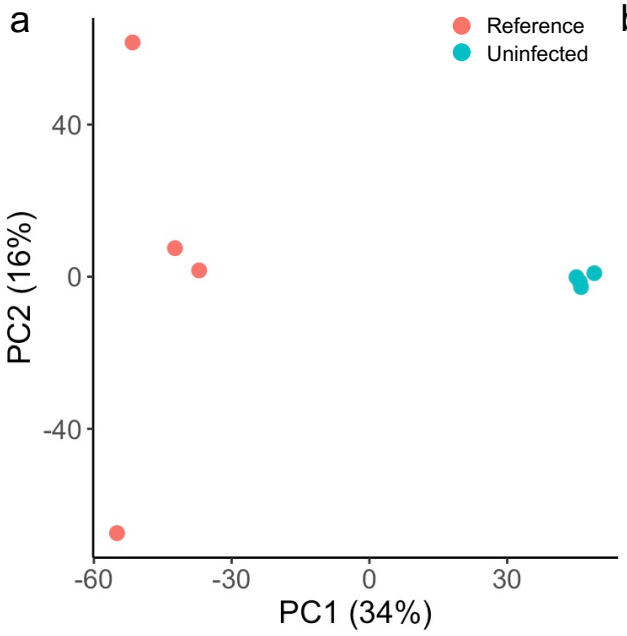
a
Reference
Uninfected
40
0
-40
PC2 (16%)
-60
-30
0
30
PC1 (34%)

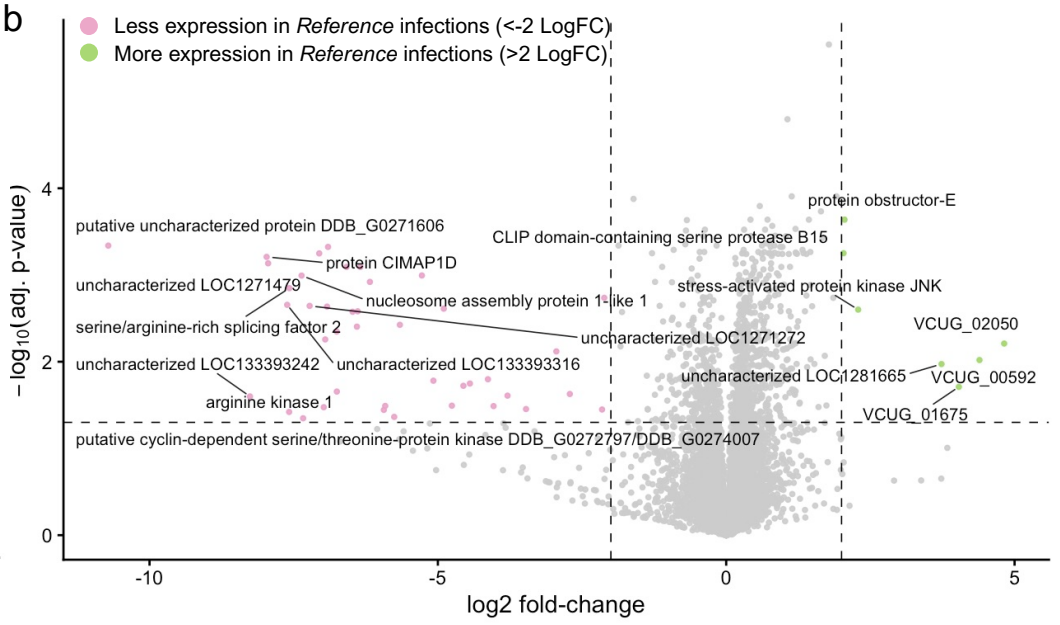
b
Less expression in *Reference* infections (<-2 LogFC)
More expression in *Reference* infections (>2 LogFC)
putative uncharacterized protein DDB_G0271606
protein CIMAP1D
uncharacterized LOC1271479
nucleosome assembly protein 1-like 1
serine/arginine-rich splicing factor 2
uncharacterized LOC1271272
uncharacterized LOC133393242
uncharacterized LOC133393316
arginine kinase 1
CLIP domain-containing serine protease B15
protein obstructor-E
stress-activated protein kinase JNK
VCUG_02050
uncharacterized LOC1281665
VCUG_00592
VCUG_01675
putative cyclin-dependent serine/threonine-protein kinase DDB_G0272797/DDB_G0274007
4
2
0
$-\log_{10}$(adj. p-value)
-10
-5
0
5
log2 fold-change

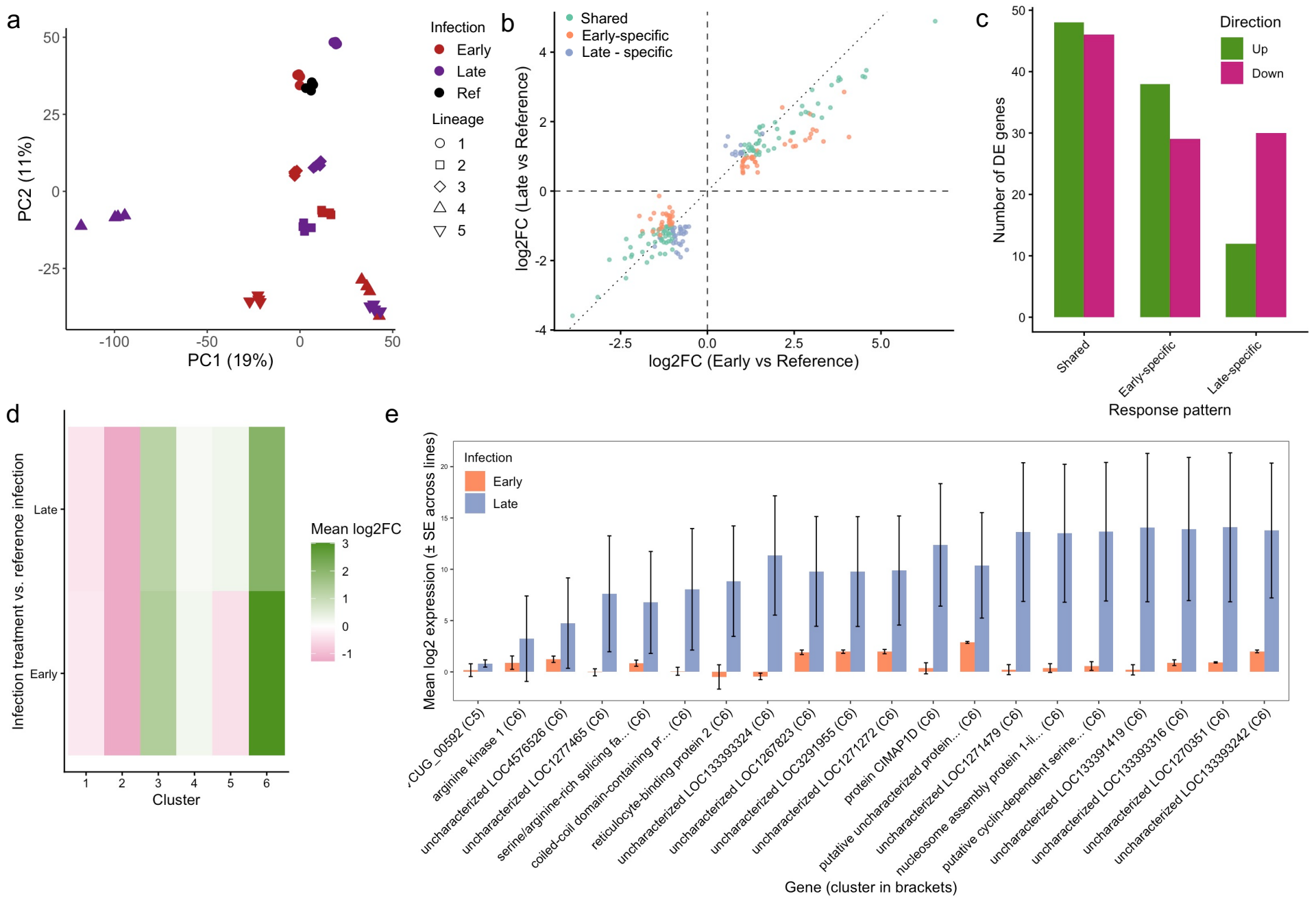
a
PC2 (11%)
PC1 (19%)
Infection
Early
Late
Ref
Lineage
1
2
3
4
5
b
Shared
Early-specific
Late - specific
log2FC (Late vs Reference)
log2FC (Early vs Reference)
c
Direction
Up
Down
Number of DE genes
Shared
Early-specific
Late-specific
Response pattern
d
Infection treatment vs. reference infection
Late
Early
Mean log2FC
Cluster
e
Infection
Early
Late
Mean log2 expression (± SE across lines)
CUG_00592 (C5)
arginine kinase 1 (C6)
uncharacterized LOC4576526 (C6)
uncharacterized LOC1277465 (C6)
serine/arginine-rich splicing fa... (C6)
coiled-coil domain-containing pr... (C6)
reticulocyte-binding protein 2 (C6)
uncharacterized LOC133393324 (C6)
uncharacterized LOC1267823 (C6)
uncharacterized LOC3291955 (C6)
uncharacterized LOC1271272 (C6)
protein CIMAP1D (C6)
putative uncharacterized protein... (C6)
uncharacterized LOC1271479 (C6)
nucleosome assembly protein 1-li... (C6)
putative cyclin-dependent serine... (C6)
uncharacterized LOC133391419 (C6)
uncharacterized LOC133393316 (C6)
uncharacterized LOC1270351 (C6)
uncharacterized LOC133393242 (C6)
Gene (cluster in brackets)

a

Co-expression modules	Early	Late	Virulence	Host exploitation	Fecundity	Envir. persistence
M9	**0.38 p=0.007**	0.01 p=0.931	-0.26 p=0.422	-0.25 p=0.437	-0.19 p=0.552	**0.68 p=0.015**
M8	0.15 p=0.308	-0.22 p=0.133	-0.25 p=0.437	-0.01 p=0.981	-0.11 p=0.727	0.37 p=0.231
M7	0.06 p=0.685	0.11 p=0.451	0.44 p=0.149	0.04 p=0.894	-0.29 p=0.361	-0.31 p=0.332
M6	**0.48 p=0.001**	0.05 p=0.720	0.30 p=0.339	0.00 p=0.993	-0.36 p=0.247	0.14 p=0.657
M5	0.23 p=0.115	0.14 p=0.349	0.36 p=0.249	0.16 p=0.609	-0.33 p=0.299	-0.23 p=0.466
M4	-0.14 p=0.342	0.08 p=0.590	0.52 p=0.085	0.41 p=0.188	0.02 p=0.961	-0.32 p=0.307
M3	-0.05 p=0.711	-0.21 p=0.154	**-0.66 p=0.020**	-0.31 p=0.326	0.35 p=0.266	0.42 p=0.171
M2	0.03 p=0.837	-0.13 p=0.370	-0.08 p=0.808	0.12 p=0.720	-0.14 p=0.671	0.12 p=0.717
M16	0.27 p=0.065	**-0.31 p=0.034**	0.18 p=0.576	-0.02 p=0.959	-0.47 p=0.126	0.22 p=0.486
M15	**0.33 p=0.020**	0.03 p=0.814	0.48 p=0.117	0.30 p=0.350	-0.37 p=0.236	-0.19 p=0.555
M14	**0.39 p=0.006**	0.15 p=0.318	0.29 p=0.368	-0.07 p=0.830	-0.11 p=0.738	0.05 p=0.874
M13	0.23 p=0.123	-0.25 p=0.084	-0.37 p=0.236	-0.27 p=0.396	-0.57 p=0.051	0.41 p=0.186
M12	0.25 p=0.090	0.00 p=0.984	-0.46 p=0.129	-0.38 p=0.226	-0.30 p=0.340	0.30 p=0.341
M11	0.12 p=0.402	-0.15 p=0.309	0.40 p=0.199	0.30 p=0.351	0.11 p=0.742	-0.05 p=0.880
M10	-0.28 p=0.059	0.16 p=0.292	0.21 p=0.507	0.30 p=0.344	0.57 p=0.052	-0.40 p=0.193
M1	-0.27 p=0.061	0.17 p=0.253	-0.07 p=0.821	-0.10 p=0.764	0.38 p=0.218	-0.17 p=0.596
M0	0.05 p=0.741	**0.32 p=0.029**	0.09 p=0.784	0.27 p=0.391	0.45 p=0.143	-0.30 p=0.348

Infection treatment / Evolved trait

Correlation: 1.0, 0.5, 0.0, -0.5, -1.0

b

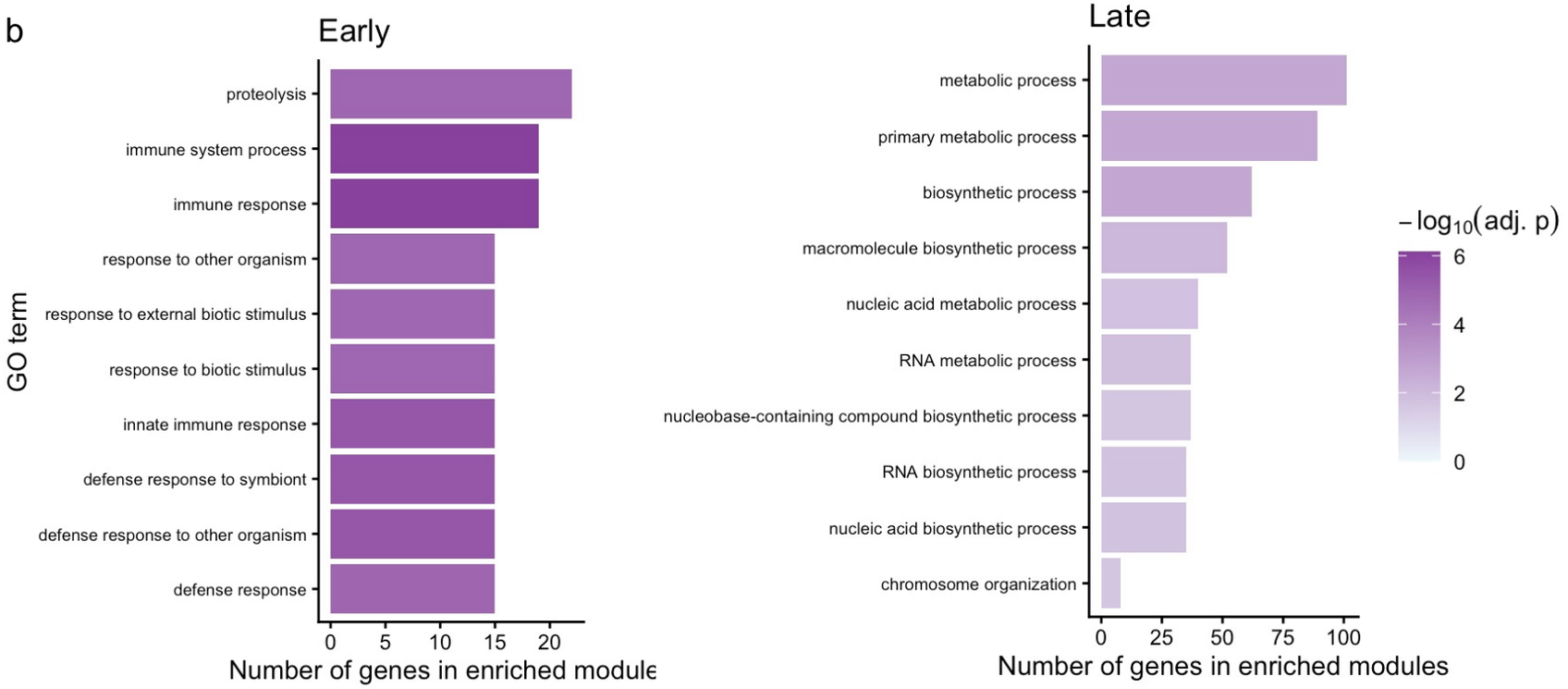

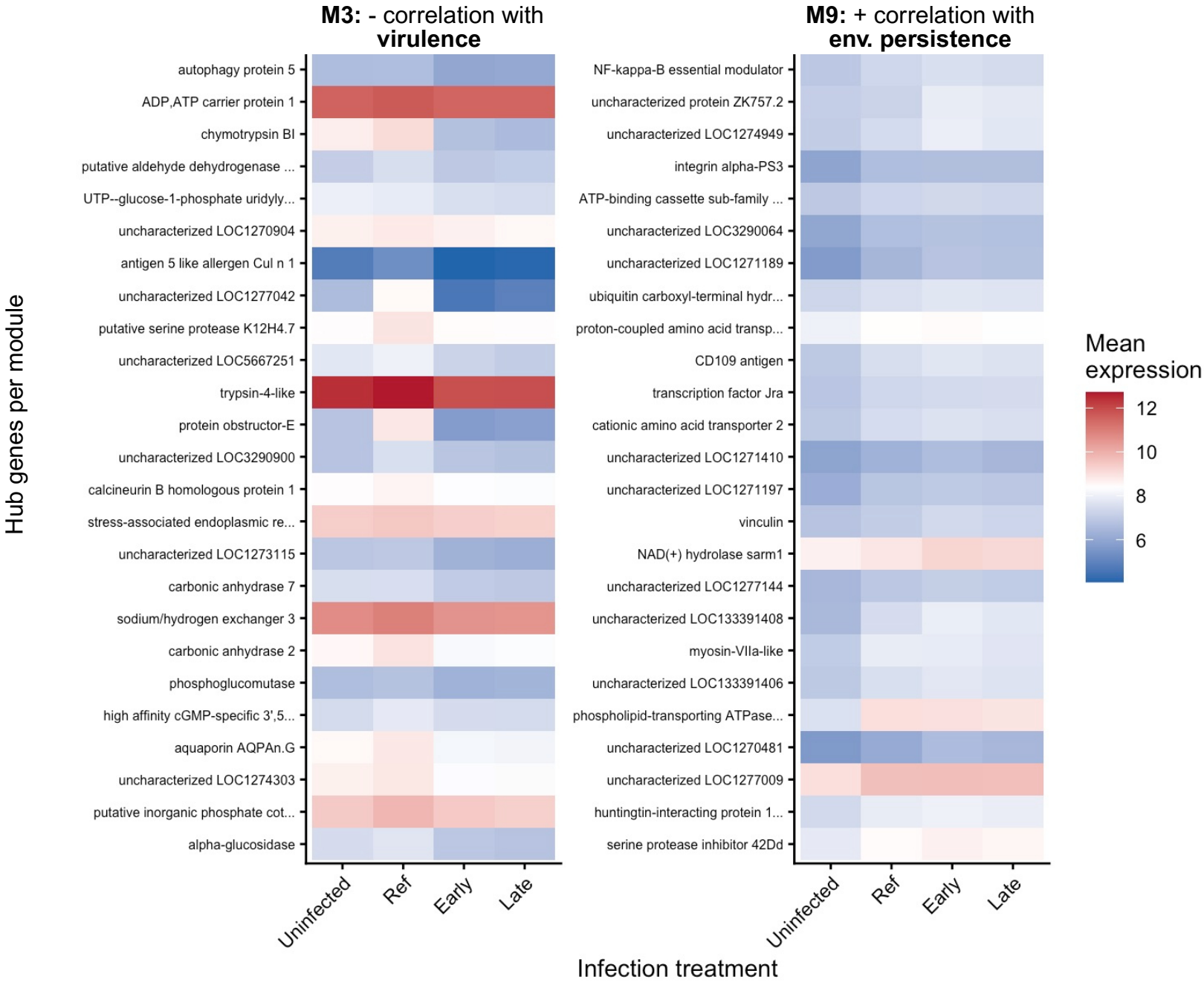
M3: - correlation with virulence
M9: + correlation with env. persistence
Hub genes per module
autophagy protein 5
ADP,ATP carrier protein 1
chymotrypsin BI
putative aldehyde dehydrogenase ...
UTP--glucose-1-phosphate uridyly...
uncharacterized LOC1270904
antigen 5 like allergen Cul n 1
uncharacterized LOC1277042
putative serine protease K12H4.7
uncharacterized LOC5667251
trypsin-4-like
protein obstructor-E
uncharacterized LOC3290900
calcineurin B homologous protein 1
stress-associated endoplasmic re...
uncharacterized LOC1273115
carbonic anhydrase 7
sodium/hydrogen exchanger 3
carbonic anhydrase 2
phosphoglucomutase
high affinity cGMP-specific 3',5...
aquaporin AQPAn.G
uncharacterized LOC1274303
putative inorganic phosphate cot...
alpha-glucosidase
NF-kappa-B essential modulator
uncharacterized protein ZK757.2
uncharacterized LOC1274949
integrin alpha-PS3
ATP-binding cassette sub-family ...
uncharacterized LOC3290064
uncharacterized LOC1271189
ubiquitin carboxyl-terminal hydr...
proton-coupled amino acid transp...
CD109 antigen
transcription factor Jra
cationic amino acid transporter 2
uncharacterized LOC1271410
uncharacterized LOC1271197
vinculin
NAD(+) hydrolase sarm1
uncharacterized LOC1277144
uncharacterized LOC133391408
myosin-VIIa-like
uncharacterized LOC133391406
phospholipid-transporting ATPase...
uncharacterized LOC1270481
uncharacterized LOC1277009
huntingtin-interacting protein 1...
serine protease inhibitor 42Dd
Uninfected
Ref
Early
Late
Infection treatment
Mean expression
12
10
8
6